THE INTERACTION OF WIND AND FIRE

(Review Article)

TOM BEER

Bushfire Research Program, CSIRO Private Bag 1, PO Mordialloc Vic. 3195 Australia

(Received in final form 15 August, 1990)

Abstract. The rate of spread of a wildfire increases markedly when a wind springs up. Why and how this happens is still not completely understood. However, by using a judicious mixture of laboratory experiments, field experiments, sensitivity analyses of existing wildfire spread models and physical reasoning it is possible to identify some features that have not been adequately considered in the past. In particular: (i) the energetics of wind-blown wildfires indicate that a fire-wind may not exist and that the wind may blow through the fire line. ii) The rate of spread of the fire-front depends on the atmospheric stability such that the fire-front speeds are 50% or more faster during winds in the 2 to 6 m/s range under unstable conditions. iii) The wind speed acting on the flame provides an upper limit to the flame propagation speed. Existing attempts to constrain the propagation rate of fire-spread models at high wind speeds appear incorrect and, iv) wind fluctuations interacting with the standing fuel generate sweeps of downward air which carry the flame into the fuel bed and directly preheat the fuel.

Notation

a	surface area of fuel,
A, B, b, c	empirical parameters,
C	specific heat of fuel,
C_p	isobaric specific heat of air ($1005\ \mathrm{J\,kg^{-1}\,K^{-1}}$)
d	diameter of cylindrical fuel element,
D	flame depth
E	empirical parameter
g	acceleration due to gravity ($9.8\ \mathrm{m\,s^{-2}}$)
G	volume of air for combustion per mass of fuel (typically $4.3\ \mathrm{m^3/kg}$)
h	vertical height of air affected by combustion
H	flame height
I	Byram intensity
k	thermal conductivity
K	von Karman's constant (0.40)
l	length scale (diameter for cylinders)
L	flame length
L_m	Monin–Obukhov length
P_1	power dissipation per metre of flame-front due to conduction
P	power dissipation per metre of flame-front due to convection
q	heat yield (17 MJ/kg)
Q_r	radiant power per unit area
s	surface area to volume ratio
t	time
T	temperature
T_f	flame temperature
u_*	friction velocity
U	ambient wind speed
U_f	fire-wind speed

Boundary-Layer Meteorology **54**: 287–308, 1991.

V	forward speed of fire front
v	fuel volume
w	fuel areal density or fuel load (typical value is 0.5 kg/m^2)
W	vertical speed of flame-tip fluid
z	height above the ground
z_o	roughness length
Z	vegetation height
α	view angle between flame tip and fuel element
β	geometric factor in convective heat transfer
ϵ	flame emissivity
ζ	zero-plane displacement
η	kinematic viscosity of air
θ	angle between flame and the vertical
θ_s	angle of slope (from the horizontal)
κ	thermal diffusivity of wood
λ	heat transfer coefficient
μ	volume of air per unit time
φ_w	wind correction factor in Rothermel model
φ_s	slope correction factor in Rothermel model
ρ	density of the fuel
ρ_a	density of air (typically 1.2 kg/m^3)
σ	Stefan-Boltzmann constant
τ	flame residence time

1. Introduction

The scientific study of wildfires, or bushfires as they are called in Australia, presents considerable challenges. The theoretician needs to consider the effects of a self-sustaining exothermic chemical reaction occurring within a combustible porous medium composed of discrete elements, possibly overlapping, of various configurations and orientations. These complexities mean that no complete physically-based model of wildfire propagation exists and wildfire-researchers, along with wildfire-fighters, rely on semi-empirical models to predict fire behaviour.

It is well known that the rate of spread of a wildfire increases markedly when a wind springs up. This is illustrated in Figure 1, taken from data generated by the meteorological tables of Beer (1990), which reproduces the predicted rates of spread for wildfire from the Rothermel (1972) model as a function of wind speed and fuel moisture content. One of the most fundamental problems in wildfire research, yet one of the least satisfactorily answered, is why and how this happens.

The simplest view conceptually is to assume that all of the heat transfer responsible for the forward propagation is due to radiation from the flame and to ascribe the increase in fire speed to geometric effects. To some extent, this reasoning must be correct. Wildfires move faster up slopes, even in the absence of wind, than on level ground. This increased rate of spread on slopes is partly due to gravity and partly due to geometry. It may be shown (Turner, 1973: Section 6.2) that the gravity effect varies as the one-third power of the slope, whereas experi-

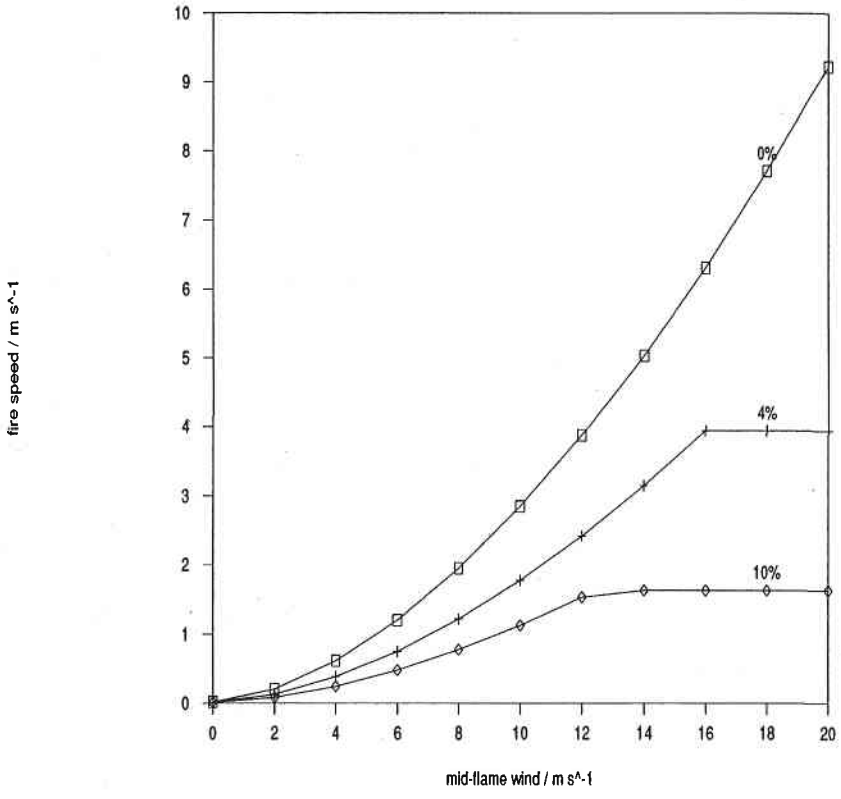

Fig. 1. Rothermel model predictions of rate of spread (km/h) of a fire-front as a function of mid-flame wind speed for fuel of 0.5 kg/m^2 dry mass 10 cm deep with surface area to volume ratio of 80 cm^{-1} with moisture content of 0, 4 and 10%.

ments on fires indicate that they increase their speed as the square of the slope. The increased spread rate on slopes must therefore be primarily a result of geometry.

The matter is not, however, so simple. If the increased rate of spread on slopes is dominated by geometry, then one would expect wildfire spread models, such as Rothermel's (1972) phenomenological model, to have similar forms for the wind and slope corrections. Rothermel (1972) uses empirical factors to account for the influence of wind and terrain slope as

$$V = V_o(1 + \phi_w + \phi_s) \tag{1}$$

where V_o is the fire spread rate in the absence of both wind and slope, φ_w is a factor that incorporates the increase due to ambient wind, and φ_s is the slope factor. These factors are of the form

$$\phi_w = AU^B \tag{2}$$

$$\phi_s = E \tan^2 \theta_s \tag{3}$$

TABLE I
Representative values of the coefficients A, B and E as a function of the surface area to volume ratio (s) at optimum values of the packing ratio

s cm^{-1}	A (for U in m/s)	B	E	Packing ratio
285	1.46	3.38	34.03	0.0020
154	2.52	2.43	29.29	0.0033
69	3.97	1.57	24.01	0.0064
40	4.77	1.17	21.03	0.0099

where θ_s is the angle between the sloping terrain and the horizontal. Values of A, B and E depend on the surface area to volume ratio (s, normally given in cm^{-1}) and on the value of the packing ratio (the proportion of the fuel volume actually covered by fuel). Values are given in Table I for fuels of various surface area to volume ratios at packing ratios that Rothermel (1972) claimed to be the optimum (i.e., associated with the maximum value of his reaction velocity).

A fire moving along level ground under the influence of a wind, U, will lean forward at an angle θ to the vertical (see Figure 8a). This angle is given by

$$\tan \theta = \frac{U}{W} \tag{4}$$

where W is the vertical velocity of the flame gases at the flame tip. If flame geometry controlled the dynamics, then θ would play an identical role to θ_s and one would expect B to have a constant value of 2 as in Equation (3). The point to note in Table I is that the changes in the value of B indicate that the flame and fire-front dynamics must involve more than just geometry.

2. Energetics

The energy balance of a propagating wildfire seems crucial to understanding its dynamics. In the following sections we treat the flame as a triangle with depth D, height H, and length L and consider the energetics of 1 m of fire-line (Figure 3a).

We shall consider the case of a fire moving in fuel with 10% moisture content with the properties given in Figure 1. The variable that characterises the severity of a wildfire is its power dissipation per unit of fire line. This quantity I, (which has units of W m^{-1}), is eponymously called the Byram intensity (Byram, 1959). It is defined in terms of the heat yield, q (in J kg^{-1}), of the burning material, the areal density, w (in kg m^{-2}), of the consumed fuel (also called the fuel load) and V (in m s^{-1}), the forward speed of the fire as

$$I = qwV, \tag{5}$$

We shall assume a heat yield, q, of 17 Mg/kg – a value appropriate to cellulose (International Critical Tables, 1929).

Dimensional reasoning can be used to relate I to the flame height, H by using the plume theory of Raupach (1990) and assuming that the flame height is the height at which the flame temperature is at some specified value. This implies a specified value of the buoyancy parameter and one finds that for a line fire, I should vary as $H^{3/2}$. In light winds, when the flame is not far from vertical this implies that I should vary as $L^{3/2}$, where L is the flame length.

Numerous field experiments have tested the relationship between I and the observed flame length (Alexander, 1982). A number of workers have used empirical regressions of the form

$$L = cI^b \tag{6a}$$

and found exponents in the range from $b = 0.46$ (Byram, 1959) to $b = 0.49$ (Nelson and Adkins, 1986). Thomas (1971) favoured the theoretically expected $b = 2/3$ but conceded that the observational data did not support it. It now appears to be common practice in the fire-research community to estimate frontal fire intensity from direct observations of flame length, based on Equation (6a) with b taken as 0.5. This value is used because experiments on different fuels lead to slightly different equations. Chandler *et al.* (1983) suggest that a suitable simplification is

$$I = 300L^2 \tag{6b}$$

where L is in m and I is in kW m^{-1}.

In section 3 of this paper, I make the point that neither flame length nor flame height will be stable observables because the fluid dynamics is such that the flame must continuously elongate and contract. Nevertheless, it appears that there is some visual averaging taking place such that different observers report similar flame lengths. The situation is analogous to that in oceanography (Beer, 1983: p. 50) where wave-height is a variable that fluctuates stochastically yet mariners consistently report the value of the third decile as the wave height.

The residence time for flames is defined by

$$\tau = \frac{D}{V} \tag{7}$$

where D is the flame depth. Anderson (1969) claimed that τ depends only on the fuel properties and proposed a formula that in SI units is

$$\tau = \frac{75600}{s} \tag{8}$$

where s is the surface area to volume ratio of the fuel (in units of m^{-1}) and τ is then given in seconds. Sneeuwjagt and Frandsen (1977) tested this relationship against their grassland fire results and, despite considerable scatter in their regres-

sion curve, claimed to have confirmed it. The combination of Equations (7) and (8) indicates that flame depth, D, increases with fire size.

Having developed empirical relationships for the size of the flame variables, it should now be possible to apportion the energy dissipation from the flame, as measured by I, between conduction, convection and radiation.

2.1 Conduction

Assume that the fuel is composed of cylinders of diameter d with thermal diffusivity κ. The residence time for the flame passing over it follows from Equation (8) because $s = 4/d$. A time scale for conductive heat transfer to a depth z is $z^2/(4\kappa)$ from basic diffusion-equation heat theory. The thermal diffusivity varies amongst wood species. Based on the data in Chandler *et al.* (1983: p. 6–8), values range from 1.4×10^{-7} m^2/s for lichen to 2.6×10^{-7} m^2/s for partly decayed white fir. For the specific heat of dry wood, a representative value of 1675 J K^{-1} kg^{-1} (0.4 cal K^{-1} g^{-1}) was used, though it varies with temperature and moisture content (Skaar, 1972).

Pilot flame ignition of wood takes place at about 600 K. There is a rapid rise in temperature behind the flame front to values that range from 850 K for small flame depths (tens of centimetres) to 1200 K for flame depths in excess of 1 m (Chandler *et al.*, 1983).

The above time scale can be used because the temperature distribution in a cylinder is very nearly the same as that in a slab whose thickness equals the diameter (Carslaw and Jaeger, 1959: p. 200). Calculations indicate that fuels of diameter less than about 10 mm will have their centres heated to ignition temperatures, a result that agrees with the foresters' rule of thumb that only fine-fuels (defined as of less than 6 mm diameter) burn readily.

The heat transfer by thermal conduction, over 1 m of fire line, from the flame to the wood with which it is in contact is $wCVdT$, in SI units of W m^{-1} where w is the fine-fuel loading, dT (assumed to be 1000 K) is the temperature difference between the flame and the wood, and C is the specific heat of wood. The total power dissipation due to conduction over 1 m of fire line is

$$P_1 = w(CdT + mL)V \tag{9}$$

where m is the fuel moisture (expressed as a fraction of the dry weight), and L is the latent heat of vaporisation of water (2.3×10^6 J kg^{-1}).

2.2. Radiation

The total power per unit area radiated from an ideal black body is σT^4 which, at a temperature of 1200 K, amounts to 118 kW m^{-2}. The emissivity of flames from typical pine fuels is in the range 0.16 to 0.28 (Anderson, 1969). This radiation is emitted to air from 2 faces whose area for 1 m of fire line numerically equals the

TABLE II

Energetics for the fuels of Fig. 1 with 10% fuel moisture content, and 17 MJ/kg heat yield

Mid-flame wind	(m/s)	0	2	4	8
V	(km/hr)	0.03	0.29	0.87	2.79
V	(m/s)	0.0083	0.081	0.24	0.775
I	(kW/m)	70.55	688.5	2040	6587.5
L	(m)	0.48	1.51	2.61	4.69
D	(m)	0.08	0.77	2.27	7.32
Heat	(kW/m)				
Conduction		7.9	77.2	228.6	738.2
Radiation		41.3	190.4	439.9	1173.9
Convection		21.3	420.9	1371.5	4675.5
Moisture content		0.1	0.1	0.1	0.1
Fuel load	(kg/m^2)	0.5	0.5	0.5	0.5
SAVR (s)	(cm^{-1})	80	80	80	80

flame length. In addition, there is one face radiating downward to the fuel, or the ground, whose emissivity is close to 1 (being composed of char) and whose area is numerically equal to the flame depth.

2.3. Convection

The heat transfer to convection, P, follows by subtraction.

Table II gives representative values for various wind speeds. The point to note from Table II is that the importance of convection in the energetics of the fire increases with the size of the fire. The reason for this can be seen by noting that

$$P = I - w(C\,dt + mL)V - \sigma T^4 D - 2\epsilon\sigma T^4 L. \tag{10a}$$

However, because both D and I are linear in V, this may be written in terms of I as:

$$P = (1 - b_1)I - b_2 I^{1/2}. \tag{10b}$$

The reason that the ratio P/I increases with fire size is that the flame radiation term becomes progressively smaller. The importance of flame radiation in the overall fire energetics decreases as the fire gets bigger.

3. The Fire-Wind

Many conceptual ideas about propagating wildfires are extrapolations from our ordinary experience with stationary fires in fireplaces. Thus, it is sometimes suggested that a reason for the increased speed of a fire-front under windy conditions is the increased oxygen supply. This seems unlikely. The argument against it is as follows. In a propagating fire, a proportion of the heat is used to heat the fuel

elements ahead of the fire and bring them to ignition. During the pre-ignition phase, volatile gases diffuse out from the interior of the fuel elements. They cannot be ignited until (i) they have mixed with sufficient oxygen to form a flammable mixture, and (ii) the mixture has a temperature above the ignition temperature. The volatiles, being warmer than their surroundings, rise and mix with air as they do so. Thus, at some height, sufficient oxygen will have been entrained to form a flammable mixture. As soon as the mixture is flammable, and the ambient temperature is greater than or equal to the ignition temperature, the mixture bursts into flame. This section will quantify this argument and show that there is always sufficient oxygen during wind-blown fires.

The success of the process described in the previous paragraph depends on the wind speed upwind of the fire. In fireplaces, and around wildfires in calm conditions, there is a relatively shallow inflow over the fire perimeter known as the fire-wind (Smith *et al.*, 1975). The fact that this wind is an inflow is evident from the inward lean of the flames. The flame radiation from both sides of the flame is predominantly directed upwards, and not towards the ground. Because the radiation absorbed by a fuel element depends on the cosine of the angle between the normal to the flame surface and the fuel element (deMestre *et al.*, 1989; see also Equations (17) and (18) of this paper), an inward leaning flame means that this angle approaches ninety degrees, and the cosine term is small. The heat transfer responsible for the forward propagation in this case must therefore come from a combination of conduction, and radiation within the fuel bed.

The air supply to the fire can be estimated by assuming that all the energy of convection is used in heating. Thus over 1 m of fire line,

$$dP = \mu \rho_a C_p dT \tag{11}$$

where we take 1005 J kg^{-1} K^{-1} as the isobaric specific heat of air C_p, and in the absence of an ambient wind use 21.3 kW m^{-1} for dP (see Table II). The air requirement is then 0.021 kg per s. As a typical density of air (ρ_a) is 1.2 kg m^{-3}, this equates to a flux (μ) of 0.018 m^3 s^{-1} of air over each 1 m of fire line.

Assuming that the cellulosic fuel undergoes complete combustion as

$$C_6H_{10}O_5 + 6O_2 \rightarrow 6CO_2 + 5H_2O,$$

stoichiometry then indicates that the combustion of 162 g of cellulose needs 192 g of oxygen. Oxygen is 21% of air by volume, which is 23% by mass. Thus 1 kg of cellulose requires 4.3 m^3 of air to burn. The calculations so far assume a fuel loading of 0.5 kg m^{-2}. Thus these calculations indicate that if there is no horizontal air motion, the air supply to burn this fuel would come from a height, h, of at least 2.15 m. Because the height of the flame is only about 0.49 m (Table II), there would need to be a drawdown of air; this cannot be. The chemical equation for combustion transforms 6 moles of oxygen to 11 moles of gaseous product so, by the universal gas law, there must be expansion or an increase in pressure by the

factor 11/6. The necessary oxygen must be supplied by turbulent mixing from an inward horizontal flow.

The strength of the fire wind can be estimated by calculating the characteristic flux of air needed to chemically maintain a particular heat source strength, and comparing this to the flux induced by convection. The stoichiometric flux (per m of fire line) is given by GwV, where G (4.3 m^3/kg) is the volumetric air requirement per kilogram of fuel. The flux induced by convection, μ, is given by $\mu = dP/(\rho_a C_p \, dT)$. Both fluxes are calculated in Table III.

When there is no ambient wind, the convective flux fails to provide sufficient air to satisfy stoichiometry and a fire-wind will be set up. The strength of the fire wind will be weak, because the two fluxes are almost in balance. The situation is different in the presence of an ambient wind. The stoichiometric constraint is then much weaker than the convective or dynamical constraint.

A numerical estimate of the strength of the fire wind requires an estimate for the height, h, of the fire wind. The argument given above implies that in the no-wind case, this will be equal to (or lower than) the flame height. In the presence of an ambient wind, assume it to be the height at which there is sufficient air to satify the stoichiometric flux. Define U_f as the speed of the fire-wind. Then for $V > U$,

$$GwV = h(U - V) \tag{12}$$

determines h. The energetics stage calculation gives the air requirements to maintain the convective plume. If the fire-wind is restricted to the height h, then there is insufficient air from the ambient wind, and there needs to be an indraw of air such that

$$(\mu - GwV)/2 = hU_f \tag{13}$$

where the factor of 2 accounts for inflow from both sides of the flame. Values of U_f so calculated are given in Table III. The important point to note is that the

TABLE III
Fluxes and fire-wind calculations for the fires of Table II.

Mid-flame wind	(m/s)	0	2	4	8
V	(m/s)	0.0083	0.081	0.24	0.775
Stoichiometric flux	(m^3/s) per metre	0.0178	0.1742	0.5160	1.6663
Convective flux	(m^3/s) per metre	0.0177	0.3490	1.1372	3.8768
Theoretical fire wind height	(m)	0.48	0.09	0.14	0.23
Inflow	(m^3/s) per metre	0.0177	0.35	1.14	3.88
Theoretical fire wind speed	(m/s)	0.0037	0.96	2.26	4.79

value of the maximum predicted fire-wind is comparable with the value of the ambient wind. One would expect this to manifest itself in field experiments. This is not the case. The National Bushfire Research Unit has conducted both field and laboratory experiments to find evidence for the fire-wind. The laboratory experiments (one of which is shown in Figure 7) consisted of match arrays burnt in a small wind tunnel. The field experiments, conducted at Harden NSW in late February 1988, consisted of three fires propagating in wheat stubble with a vertical line of smoke flares placed such that the fire propagated underneath it. Both field and laboratory experiments failed to detect evidence of a fire-wind ahead of the fire-front.

On the basis of the above calculations, there seems little reason to expect a fire-wind in the case of a wind-driven fire, and attempts to impose one have, in the past, led to unrealistic airflow patterns such as those of Nelson (1986: Figure 2) and Grishin *et al.* (1984: Figure 1). The theoretical airflow patterns of these authors are depicted in Figure 2, on which there has also been superimposed a schematic of the results from the wheat stubble burns at Harden. The two are in conflict. The theoretical flow assumes that air for combustion comes from the lee of the flame. The experimental results, in conjunction with the above calculations, imply that there is sufficient air emanating from behind the fire.

Raupach (1990) has used similarity analyses to arrive at similar conclusions. His method predicts the fire-wind to be

$$U_f = 0.166\left(\frac{gI}{\rho_o C_p T}\right)^{1/3}. \tag{14}$$

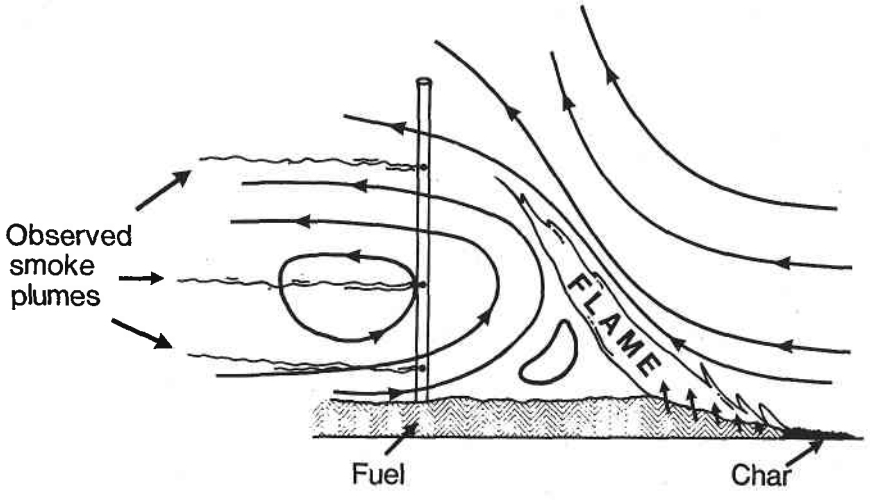

Fig. 2. Schematic diagram showing the (incorrect) two-dimensional flow in the vicinity of a wildfire suggested by various authors (see text) compared with the observations from smoke bombs placed on a tower ahead of the fire.

Though this formula produces quantitative values that differ somewhat from those in Table III, the qualitative result, namely that the fire wind reaches appreciable values only for very intense fires, is the same in both cases. As Raupach (1990) says: "The action of the fireline as a windbreak is therefore weak, except for strong fires".

If we view the fire as a two-dimensional line, then we are confronted by a paradox. The National Bushfire Research Unit's experiments indicate that an observer standing downwind of, and facing, a straight wind-driven fire-front will feel a wind on his face rather than his back. (He may also feel a great deal of radiant heat on his face, but that is irrelevant to the present argument.) Simple fluid dynamical reasoning indicates that this is impossible in two-dimensional flow. The hot air of the plume acts as a barrier to the passage of the ambient wind, which must be entrained into the plume. No air can thus propagate ahead of a two-dimensional fire, and mass-continuity thus requires a fire-wind to be generated ahead of the fire, so that the observer ahead of a fire should feel the wind on his back and not on his face.

The resolution of this paradox comes from the three-dimensional nature of the flame-front. A flame front advancing towards an observer will not be a uniform, changeless sheet of flame. It will consist of peaks and troughs which, incidentally, greatly complicate the field measurement of the flame height. In field experiments, there is a temptation to ascribe these peaks and troughs to inhomogeneities in the fuel. This is incorrect. A uniform fuel array, such as a line of vertical matches, when lit over a long line, has a flame that breaks into peaks and troughs. The peaks and troughs are manifestations of the thermal instability of a fluid (i.e., the hot gases comprising the flame and the plume above it) when a light fluid composed of hot combustion products is overlain by a heavier one (cold air).

Figure 3 depicts an idealised conception of the interaction between an ambient wind and a flame. Viewed from the side (Figure 3a), the visible flame is triangular

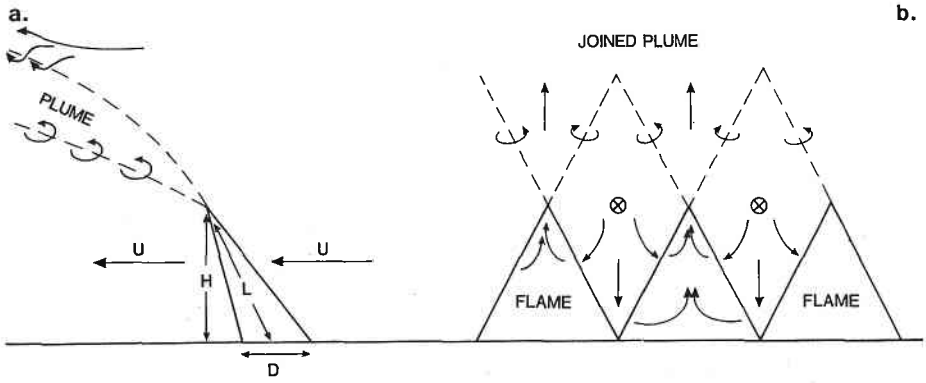

Fig. 3. Idealised conception of the interaction between an ambient wind and a flame-front viewed (a) perpendicular to the direction of flame spread and (b) along the direction of flame spread.

with a plume of hot gases and particulates emanating from its tip. This plume increases in size due to entrainment of air (depicted by curved arrows). The structure when viewed from behind the fire front is more complex (Figure 3b). The flame peaks correspond to updraught regions, and the troughs to downdraughts. The plumes from each flame peak will eventually merge, but there remain unaffected regions – depicted as diamond shapes in Figure 3b – through which ambient air can pass unaffected.

Though this 'window' picture of how the ambient wind finds its way through the fire-front is crude, it is a marked improvement on Figure 2, which assumes (incorrectly) that flames follow mean streamlines. The 'window' picture obscures the fact that the whole pattern is dancing around in time and space, causing the streamlines and particle paths of the flames and the ambient air to be inextricably entwined.

4. Wind Profiles

It has been assumed so far that a single mid-flame wind speed can be used to characterise the flames' response to the wind. In actual fact, the wind speed $U(z)$ is a function of vertical distance from the ground.

In a neutrally stable atmosphere, the surface-layer mean wind as a function of height is given by

$$U = \frac{u*}{K} \ln \frac{(z - \zeta)}{z_o} \tag{15}$$

where $u*$ is the friction velocity, K is von Karman's constant which has a value of 0.40, z_o is the roughness length and ζ is the zero plane displacement. Albini and Baughman (1979) used this relationship, with z_o and ζ related to the vegetation height Z by $\zeta = 0.64\ Z$ and $z_o = 0.13\ Z$. They produced a graph linking (i) the ratio of the average windspeed on the flame to the windspeed at a height of 20 ft (6.1 m – the standard anemometry height for US land management agencies; the meteorological standard height is 10 m), ii) the height of the fuel bed, Z and (iii) the ratio of the flame extension above the fuel bed to the height of the fuel bed.

Though this approach offers the useful rule-of-thumb that for short-grass fuels the mid-flame wind speed is 0.4 times the wind speed at 6.1 m, there are a number of weaknesses; namely:

(a) The rule-of-thumb refers to mean winds, which correspond to about 30-min averages.
(b) Garratt (1978, 1980) found that the logarithmic profile is not established until about $3Z$ to $8Z$ above the zero-plane, depending on the density of the vegetation.
(c) The logarithmic profile of Equation (15) is valid only under neutral stability.

Behind a fire that has been propagating for longer than 30 minutes (and thus describable by a mean wind), the extensive burnt ground should provide sufficient vertical heating that one should use the form of the mean wind profile appropriate to unstable conditions.

The mid-flame wind profile under non-neutral stability was examined by Durre and Beer (1989) who found that estimates of the 2 m wind speed during fires were improved when stability was incorporated. They used the Monin–Obukhov length, L_m, which is positive in stable conditions, negative in unstable conditions, and infinite in neutral conditions. Its inclusion alters the vertical dependence of the wind speed. Accurate estimates of the Monin–Obukhov length are difficult to make, but Durre and Beer (1989) found that in unstable conditions the formula

$$L_m = -\frac{U^3}{15} \tag{16}$$

with units of m s^{-1} for U and metres for L_m worked very well as a rule-of-thumb. It does so for two reasons. The first is that the number 15 in Equation (16) incorporates values of the surface roughness and heat flux that are appropriate to days of high fire danger. The second reason is that the ratio of the wind speed at 2 m to that at 10 m is only weakly dependent on L, especially for large values of z_o. A large discrepancy in L will still lead to reasonable estimates of the mean wind speed ratio.

Figure 4 (Durre, 1989) illustrates the changes in the predicted rate of spread that are obtained when stability via Equation (16) is incorporated. These changes arise from the fact that the wind speed is observed at a height of either 10 m or 20 ft, but the Rothermel (1972) fire-front rate of spread algorithm is based on mid-flame height wind speed. Identical 10 m wind speeds will produce different mid-flame height wind speeds depending on the stability conditions. Figure 4 illustrates that at low wind speed, there is little change from the rate of spread under neutral conditions because the fire moves slowly. At high wind speeds there

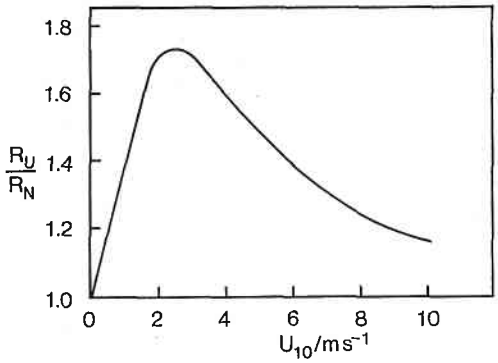

Fig. 4. The ratio between the predicted rate of fire-front spread in an unstable atmosphere (R_u) and the predicted rate of spread in a neutral atmosphere (R_N) as a function of wind speed at 10 m height.

is little change because high winds promote mechanical mixing that forces the atmosphere to neutral stability. The greatest changes occur in the 2 to 4 $m\,s^{-1}$ wind speed range.

5. Maximum Spread Rates

There is considerable uncertainty as to whether the rate of spread of a wildfire continues to increase as the wind increases, whether there is a limiting rate of spread, or whether there is a maximum rate of spread at a critical wind speed above which the rate of spread starts to decrease. McArthur (1968) found evidence for a decline in spread rate with increasing wind speed at wind speeds above 50 $km\,hr^{-1}$ (13.9 $m\,s^{-1}$) during the Tasmanian fires of 1967. Cheney (1981), commenting on these findings, notes that they occurred in sparse grasslands and there is no evidence that very high wind speeds reduce the rate of spread in heavy pastures or in forest fires.

The National Bushfire Research Unit conducted wind tunnel tests in which regular arrays of 41.75 mm high match splints (i.e., matchsticks without the ignitable heads) were burnt in a wind tunnel. The variation of fire speed with wind for single rows of match splints is shown in Figure 5. At high wind speeds, the matches were very difficult to set alight but once alight, the rate of spread continued to increase as the wind speed increased. These wind tunnel results support Cheney's view – when there is a regular supply of fuel, the spread rate continues to rise as the wind speed increases. The rate of spread decreases in sparse fuels because of the difficulty in getting an isolated fuel element alight in a strong wind.

Nevertheless, McArthur's observation was widely circulated within the wildfire community and was influential in Rothermel's (1972) setting an upper limit to the wind multiplication factor in his model. This can be seen in Figure 1 at high wind speeds and high fuel moistures where the rates of spread remain constant. Rothermel (1972) did this by identifying a critical wind speed and treating the predicted rate of spread at this critical wind speed as the maximum permissible rate of spread. The magnitude of this critical wind speed was determined by assuming that the interaction between the wind and the flame angle is dependent upon the ratio of their respective energy dissipation rates.

Though it is not evident in Figure 1, this procedure leads to anomalies for certain fuel parameters, in that the model predicts that the wildfire spread rate V exceeds the mid-flame wind speed, U: $V > U$. There seems to be no explicit mention in the literature that the wind speed, U, provides an upper limit to the fire-front rate of spread. This may be because in calm conditions it is obvious that the fire moves faster than the wind. However, as we have previously mentioned, the heat transfer in this case is radiation through the fuel bed and the visible manifestation of $V > U$ is a flame that leans inwards, away from the direction in which the fire moves. At high wind speeds, wildfire flames lean forward (i.e., $V < U$), and can be very close to the ground. The heat transfer is through flame

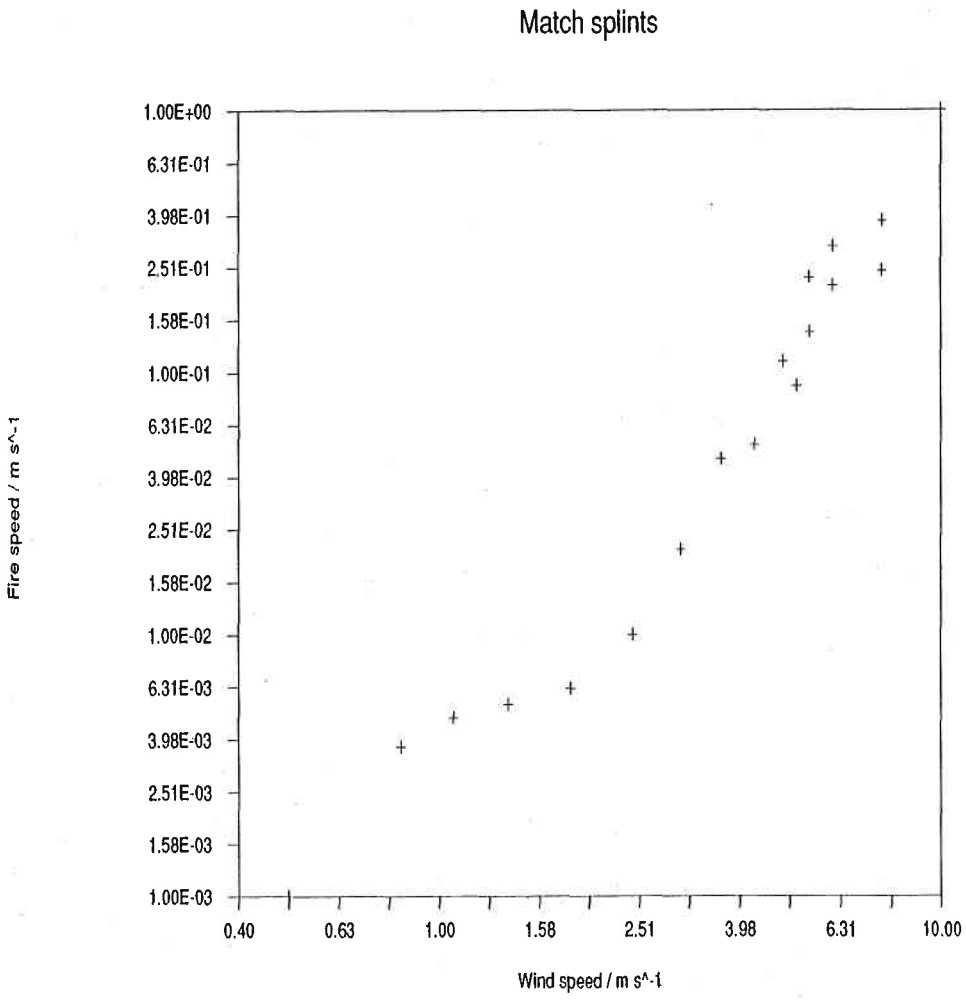

Fig. 5. Observed speed of a flame propagating down a single line of 4.175 cm high Australian match splints as a function of wind-tunnel speed. Note the use of logarithmic scales for the axes.

radiation – and possibly direct advection of hot air. The only other way that a fire could have its spread rate, V, greater than the wind speed, U, controlling the flame is if the fire spread is through "spotting." This term is used to describe burning embers being carried by the wind, settling and igniting the surface on which they settle. Because of the vertical increase of wind speed, a hot ember can move into a region of faster flow and be carried along faster than the wind at the flame. However, existing fire spread models specifically exclude spotting.

Figure 6 illustrates the anomalies that occur in the Rothermel (1972) formulation. The figure, whose axes are speed and fuel moisture content (FMC), plots the boundaries for which $V = U$ as solid lines. Fuel parameters follow those in Fig. 1 except that a 50 cm depth of fuel was used. Also shown on the figure as a dashed line is the plot of critical wind speed as a function of FMC. The solid lines

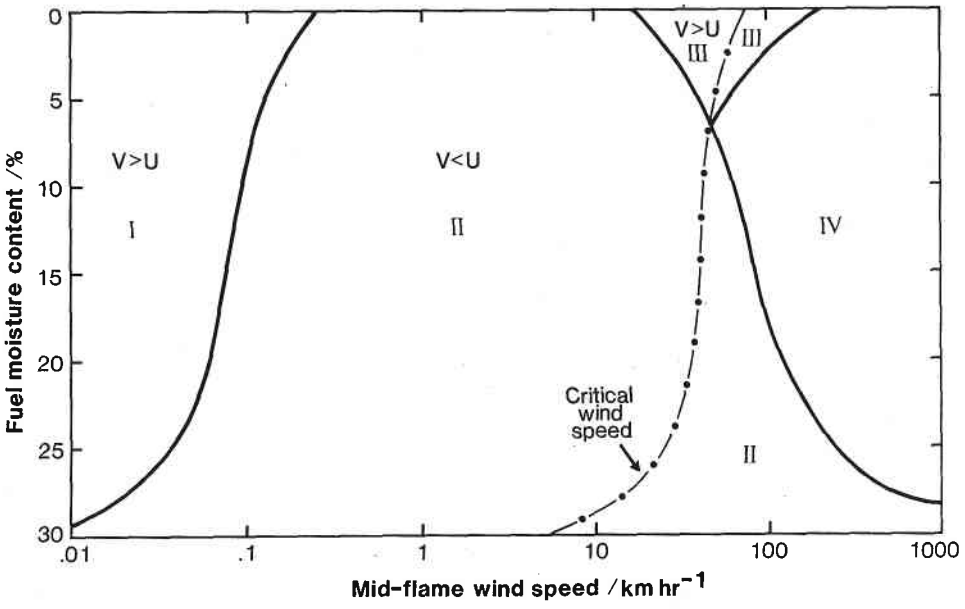

Fig. 6. The critical wind speed (dashed line) according to Rothermel (1972) as a function of fuel moisture content for fuels of depth 50 cm, surface area to volume ratio of 80 cm^{-1} and fuel load of 0.5 kg/m^2. In regions I, III and IV, the Rothermel model, before using the critical wind speed, predicts a fire-front rate of spread that exceeds the mid-flame wind speed. Limiting the spread rate by using the critical wind speed reduces the spread rate in region IV to below the wind speed, but the spread rate in region III continues to exceed the wind speed.

divide the figure into four regions, indicated by roman numerals. Region I consists of fires in calm conditions for which the model predicts $V > U$. Within region II, $V < U$.

If it is assumed that there is no cutoff to the rate of spread (i.e., the critical wind speed is taken as infinite), then both regions III and IV have $V > U$. Introducing a critical wind speed, as advocated by Rothermel (1972: Eq. 87), decreases the speeds in region IV so that $V < U$ in this region, but maintains an area, denoted by region III within which $V > U$.

The shape of the leftmost solid line is set by the choice of the moisture coefficient of extinction (30% in this example). The similarity in shape between the dashed line and this solid line which lies between regions I and II indicates that the critical wind speed approach is based on extrapolating flame characteristics appropriate to the $V = U$ boundary at low wind speeds to the limiting value of spread rate as found by McArthur (1968). The results of Figure 6 further indicate that this is not appropriate, and that the proper criterion for limiting spread rate is the requirement that $V < U$.

6. Fluctuations in Wind

The above discussion has dealt with a mean wind. The environmental wind fluctuates in both direction and speed, with increased instability of the air implying greater fluctuations. Albini (1982) examined the effects of wind fluctuations on a fire that is driven completely by flame radiation and found that the only observable effect was a billowing of smoke as the fire alternately races and pauses in response to the low-frequency variations in windspeed. In fact there are other more significant effects.

Figure 7 is a photograph taken of the combustion of a line of matches whose heads had previously been ignited. There are seven matches in each row of the line. The structure in the background is a holder for incense sticks positioned so that their smoke indicates the direction of air movement. It is noteworthy that a

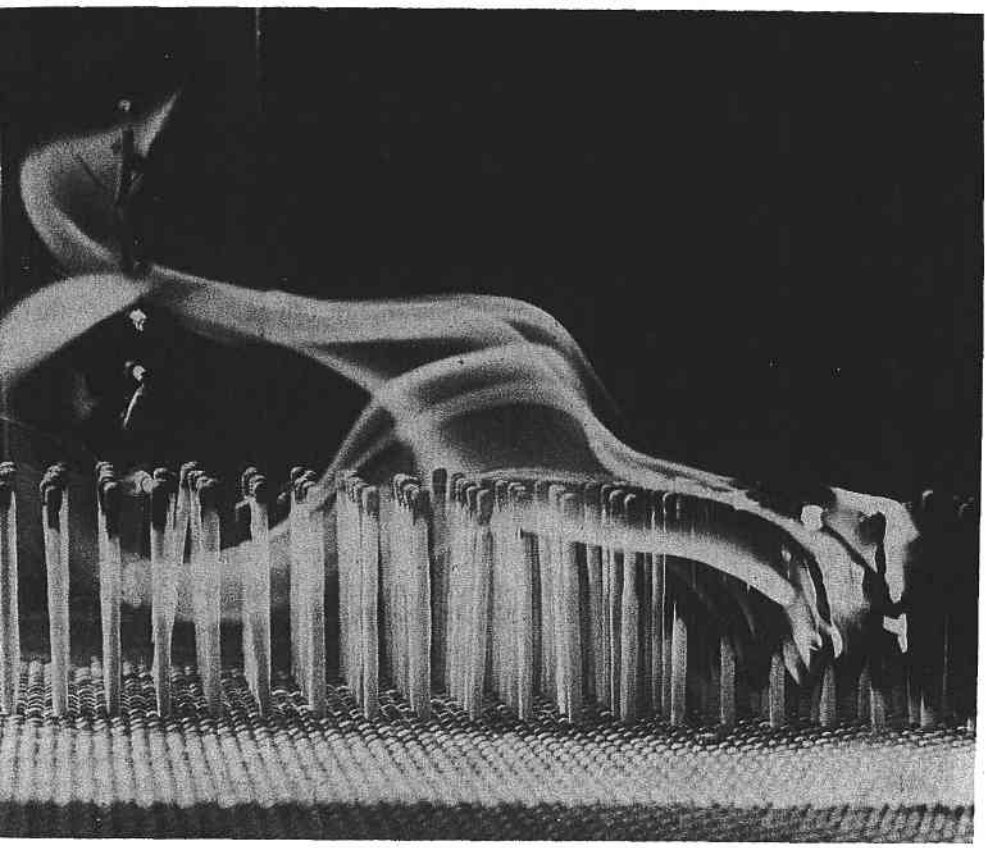

g. 7. Photograph of a laboratory experiment on a row of matches demonstrating advective preating in which the flame penetrates the fuel bed ahead of the main fire front. The structure to the ft is a holder for incense sticks positioned so that their smoke indicates the direction of air movement. The smoke at match-top height is in the direction of the wind.

substantial part of the flame is within the fuel-bed and therefore acting to pre-heat the fuel bed directly. We shall call this advective pre-heating. It showed up for 3 sec out of the 20 sec for which the experiment was photographed.

Advective pre-heating differs from the phenomenon that Chandler *et al.* (1983: p. 14) call flame trailing. As a youngster, I used to call it flame streaming and could observe it by gently (and uniformly) blowing on a candle flame so that the flame no longer moved upward but hung like a flag on the lee side of the candle-wick. Flame trailing occurs at high winds when the flame no longer lifts from the fuel bed. The increase in slope of the fire-speed versus wind speed curve of Figure 5 that occurs at about $2\,m\,s^{-1}$ is a result of flame trailing. Advective pre-heating occurs for any wind speed and is a result of fluctuations in vertical wind speed induced by the presence of the fuel. The short sweep of downward moving air flattens the flame into the fuel bed as in Figure 7. While the flame is in the fuel bed, the heat transfer mechanism from advective pre-heating is the same as that of flame trailing.

The photograph of Fig. 7 was taken during a relatively uncontrolled experiment. The matches were in a perspex-walled box with no lid, and the airflow was generated by using an ordinary domestic fan to suck the air through the box. When the experiment was repeated in a small wind tunnel with a lid and a controlled (i.e., constant) airflow, there was no evidence of such advective pre-heating. I believe that this photograph is a laboratory visualisation of the phenomenon likely to occur in a fuel canopy – i.e., the presence of short, intermittent gusts of downward moving air that originate in the boundary layer well above the surface and penetrate into the canopy. Finnigan and Raupach (1987) note that in a corn crop, these sweeps occur only about 6% of the time whereas they were observed about 12% of the time in a model canopy situated in a wind tunnel. These durations are consistent with our upper bound of 15% of the time in a match array, though it must be conceded that the fire itself has a vertical velocity scale that is liable to modify the canopy gusting process substantially.

Raupach *et al.* (1989) consider these downward sweeps of air to arise from the wind shear at the top of the canopy. If this is the case (and it is by no means certain that it is), then the charred standing matches behind the flame of Fig. 7 must play a strong role in setting up the conditions for advective pre-heating. In a crop fire or a grass fire, the fuel is totally consumed and no canopy remains to generate a shear instability. However, the mechanism should be important in forest fires where the litter burns but the trees remain standing. The uncertainty in the role of the canopy-based gusting arises because it is possible that the fire itself generates the fluctuations in vertical wind velocity so that heat can be dispersed downward from the flame sheet to the unburnt fuel ahead of the fire.

To quantify the respective roles of radiant pre-heating and advective pre-heating from the flame, consider the heat upon an infinitesimal fuel element, standing vertically, due to a flame of length L which makes an angle θ with the vertical. Consider a fuel element a distance L from the base of the flame, as in Fig. 8a.

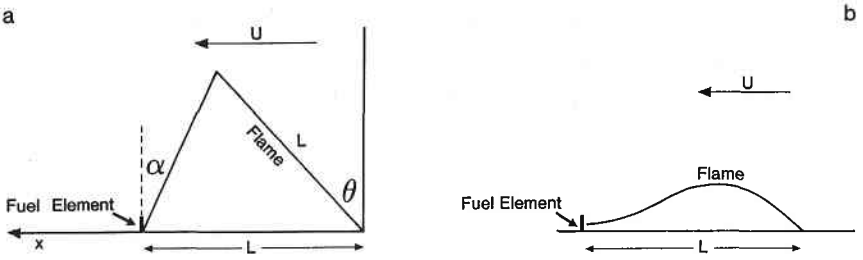

Fig. 8. (a) Wind effects lean the flame forward and increase the radiant heat to a fuel element; (b) Fluctuations in the wind can result in advective pre-heating when the flame penetrates the fuel bed.

The radiant heat per unit area upon this element is (McGuire, 1953)

$$Q_r = \epsilon\sigma T_f^4 \cos\alpha \tag{17}$$

where

$$\cos\alpha = \frac{\cos\theta}{\sqrt{2(1-\sin\theta)}}. \tag{18}$$

When the fuel element of surface area a and volume v is immersed in flame of temperature T_f, as in Figure 8b, a heat balance on the element, equating the change in heat capacity with the heat loss yields (Eckert and Drake, 1959: p. 76–77)

$$\rho C v \frac{dT}{dt} = -\lambda a (T - T_f) \tag{19}$$

where ρ is the density of the fuel, C its specific heat capacity and λ the heat transfer coefficient. Combining the advective and radiant heat per unit area, one obtains a heat balance equation:

$$\frac{\rho C}{s}\frac{dT}{dt} + \lambda T = \frac{Q_r}{2} + i\lambda T_f \tag{20}$$

where $s = a/v$ and the variable i is an intermittency parameter whose value is about 0.1 indicating that the fuel element is in the flame about 10% of the time. The radiant pre-heating term Q_r has to be halved because it is only the forward face of the surface area a that receives the radiant heat.

Boundary-layer heat transfer coefficients for leaves during forced convection depend on the thermal diffusivity, κ, the kinematic viscosity, η and the specific heat and density of air (Finnigan and Raupach, 1987) as

$$\lambda = 2\beta\rho_a C_p \left(\frac{\kappa^{2/3}}{\eta^{1/6}}\right)\left(\frac{U}{l}\right)^{1/2} \tag{21}$$

where the length scale for heat transfer, l, is the leaf dimension. Extrapolating

this result to vertical cylinders implies that l can be identified as the diameter. Finnigan and Raupach (1987) suggest that in real canopies, β has a value of 1.3, whereas Pearman *et al.* (1972) found β to be 1.08 for metal disks under ambient winds. These values contrast with the normal flat-plate engineering practice in which β is about 0.7.

The heat received from the two sources is equal when

$$l = \frac{4\beta^2 i^2 \rho_a^2 C_p^2 \kappa^{4/3} U}{\eta^{1/3} (\epsilon \sigma T_f^3)^2}. \tag{22}$$

The term $\rho_a C_p \kappa^{2/3} / \eta^{1/6}$ has a slight temperature dependence and ranges from a value of 5.9 at 300 K to 5.2 at 1200 K. Using an average value of 5.5 and taking $\beta = 1.3$, $i = 0.1$, $\epsilon = 0.28$, $T_f = 1200$ K and $\sigma = 5.67 \times 10^{-8}$ W m^{-2} K^{-4}, then $l = 2.717\ U$, where l is in mm and U is in m/s. The meaning of this is discussed below.

Recall that the ignition temperature for flames is lower during pilot ignition (i.e., direct flame contact). During periods of advective pre-heating, a substantial amount of the volatile gases between the flame base and the flame tip will be ignited earlier than they would have been with radiant heating. Fuels with diameter below l will have their energetics dominated by advective pre-heating. Fuels with larger diameters will have their energetics dominated by radiation.

It is significant, in the light of the break in slope depicted in Figure 5 at a wind speed of about 2 m/s, that substituting $U = 2.2$ m/s yields $I = 6$ mm – the cutoff limit for fine fuels. It seems that at low wind speeds, radiation dominates and advective pre-heating is important only for very fine fuels. At a wind speed of about 2 m/s, advective pre-heating becomes important for all fuels that take part in the flame propagation, in other words, those of diameters below 6 mm. In fact, the matches used to obtain the data of Figure 5 had $l = 2.19$ mm. Because of the numerous uncertainties in the values used to estimate l, it is probably appropriate merely to note that advective preheating (for which i is about 0.1) starts to dominate at about the same wind speed that flame trailing (for which i is unity) starts.

7. Conclusion

We are still unable to produce a set of differential equations and be confident that they are a realistic representation of the physical processes responsible for the spread of a wildfire subject to an ambient wind. Nevertheless, by using a mixture of laboratory experiments, field experiments, sensitivity analyses of existing wildfire spread models, and physical reasoning, it is possible to identify some features that any such equations would need to incorporate. These include:

(i) The three-dimensional nature of the airflow around and through a fire-line.
(ii) The dependence of the rate of spread of the fire-front on the atmospheric

stability which may itself be modified as a result of heating as upwind air passes over previously burnt areas.

(iii) An upper limit to the fire-front rate of spread that is determined by the wind speed affecting the flames.

(iv) Wind fluctuations resulting in advective pre-heating of fuels at low wind speeds.

(v) Flame trailing into the fuel bed at high wind speeds.

Acknowledgements

The author wishes to acknowledge the helpful comments of Dr. M. Borgas, Mr. R. Rothermel and Dr. M. Raupach.

References

Albini, F. A.: 1982, 'Response of Free-Burning Fires to Nonsteady Wind', *Combust. Sci. Tech.* **29,** 225–241.

Albini, F. A. and Baughman, R. A.: 1979, 'Estimating Windspeed for Predicting Wildland Fire Behavior', Research Paper INT-*221*, USDA Forest Service, Ogden, Utah.

Alexander, M. E.: 1982, 'Calculating and Interpreting Forest Fire Intensities', *Can. J. Bot.* **60,** 349–357.

Anderson, H. E.: 1969, 'Heat Transfer and Fire Spread', Report INT-69, USDA Forest Service, Ogden, Utah.

Beer, T.: 1983, *Environmental Oceanography*, Pergamon Press, Oxford.

Beer, T.: 1990, *Applied Environmetrics Meteorological Tables*, Applied Environmetrics, Balwyn.

Byram, G. M.: 1959, 'Combustion of Forest Fuels', in K. P. Davis (Ed.), *Forest Fire Control and Use*, McGraw-Hill, New York.

Carslaw, H. S. and Jaeger, H. W.: 1959 *Conduction of Heat in Solids*, 2nd edn., Clarendon Press, Oxford.

Chandler, C., Cheney, P., Thomas, P., Trabaud, L. and Williams, D.: 1983, *Fire in Forestry*, Volume 1, John Wiley & Sons, New York.

Cheney, N. P.: 1981, 'Fire Behaviour', in A. M. Gill, R. H. Groves, and I. R. Noble (eds.), *Fire and the Australian Biota*, Australian Academy of Science, Canberra. pp 151–175.

De Mestre, N. J., Catchpole, E. A., Anderson, D. H. and Rothermel, R. C.: 1989, 'Uniform Propagation of a Planar Fire Front without Wind', *Combust. Sci. Tech.* **65,** 231–244.

Durre, A. M.: 1989, 'Mid-flame Wind Speed and the Rothermel Rate-of-Spread', in *Proc. 8th Biennial Conf. Simulation Soc. Aust.*, Canberra.

Durre, A. M. and Beer, T.: 1989, 'Wind Information Prediction Study: Annaburroo Meteorological Data Analysis', Technical Paper 17, Division of Atmospheric Research, CSIRO, Australia.

Eckert, E. R. G. and Drake R. M. Jr.: 1959, *Heat and Mass Transfer*, McGraw-Hill, New York.

Finnigan, J. J. and Raupach, M. R.: 1987, 'Transfer Processes in Plant Canopies in Relation to Stomatal Characteristics'. In: E. Zeiger, G. D. Farquhar, and I. R. Cowan (eds.), *Stomatal Function*, Stanford University Press, Stanford, CA, pp. 385–429.

Garratt, J. R.: 1978, 'Flux Profile Relations above Tall Vegetation', *Q. J. Roy. Meteorol. Soc.* **104,** 199–211.

Garratt, J. R.: 1980, 'Surface Influence upon Vertical Profiles in the Atmospheric Near-Surface Layer', *Q. J. Roy. Meteorol. Soc.* **106,** 803–819.

Grishin, A. M., Gruzin, A. D. and Gruzina, E. E.: 1984, 'Aerodynamics and Heat Exchange between the Front of a Forest Fire and the Surface Layer of the Atmosphere', *J. Applied Mech. & Tech Phys.* **25,** 889–894.

International Critical Tables, 1929: Volume 5, p. 167, McGraw-Hill, New York.
McArthur, A. G.: 1968, 'The Tasmanian Bushfires of 7th February 1967, and Associated Fire Behaviour Characteristics', in *Conf. Papers, 2nd Aust. Natl. Conf. on Fire*, Sydney, pp. 25–48.
McGuire, J. H.: 1953, 'Heat Transfer by Radiation', Fire Research Special Report No. 2, H.M.S.O., London.
Nelson, R. M.: 1986, 'Measurement of Headfire Intensity in Litter Fuels', in A. L. Koonce, (ed.), *Prescribed Burning in the Midwest*, University of Wisconsin, Stevens Point.
Nelson, R. M. and Adkins, C. M.: 1986, 'Flame Characteristics of Wind-Driven Surface Fires', *Can. J. For. Res.* **16,** 1293–1300.
Pearman, G. I., Weaver, H. L. and Tanner, C. B.: 1972, 'Boundary Layer Heat Transfer Coefficients under Field Conditions', *Agric. Meteorol.* **10,** 83–92.
Raupach, M. R.: 1990, 'Similarity Analysis of the Interaction of Bushfire Plumes with Ambient Winds', *Math. & Comput. Modelling* (in press).
Raupach, M. R., Finnigan, J. J. and Brunet, Y.: 1989, 'Coherent Eddies in Vegetation Canopies', *Proc. Fourth Australasian Conf. Heat Mass Transfer*, Christchurch, New Zealand, pp. 75–90.
Rothermel, R. C.: 1972, 'A Mathematical Model for Predicting Fire Spread in Wildland Fuels', Research paper INT–115, USDA Forest Service, Ogden Utah.
Skaar, C.: 1972, *Water in Wood*, Syracuse University Press, Syracuse, p. 140.
Sneeuwjagt, R. J. and Frandsen, W. H.: 1977, 'Behaviour of Experimental Grass Fires vs. Predictions based on Rothermel's Fire Model', *Can J. For. Res.* **7,** 357–367.
Smith, R. K., Morton, B. R. and Leslie, L. M.: 1975, 'The Role of Dynamic Pressure in Generating Fire Wind', *J. Fluid Mech.* **68,** 1–19.
Thomas, P. H.: 1971, 'Rates of Spread of Some Wind-Driven Fires', *Forestry*, **44,** 155–175.
Turner, J. S.: 1973, *Buoyancy Effects in Fluids*, University Press, Cambridge.
Yih, C. S.: 1977, *Fluid Mechanics – A Concise Introduction to the Theory*, Corrected edition, West River Press, Michigan.